Effect of binder materials on cycling performance of Fe$_2$O$_3$ electrodes in alkaline solution

Hiroki Kitamura [a], Liwei Zhao [b,∗], Bui Thi Hang [c], Shigeto Okada [b], Jun-ichi Yamaki [b]

[a] Interdisciplinary Graduate School of Engineering Sciences, Kyushu University, 6-1 Kasuga-Koen, Kasuga 816-8580, Japan
[b] Institute of Materials Chemistry and Engineering, Kyushu University, 6-1 Kasuga-Koen, Kasuga 816-8580, Japan
[c] International Training Institute for Materials Science, Hanoi University of Science and Technology, 1 Dai CO Viet Road, Hanoi, Viet Nam

ARTICLE INFO

ABSTRACT

To investigate the effects of binder materials on the electrochemical properties of Fe$_2$O$_3$ electrodes in alkaline solution, four different materials were applied as binders: polytetrafluoroethylene (PTFE), polyvinylidene fluoride (PVDF), polyethelene (PE), and poly tetrafluoroethylene-co-vinylidene (P(TFE-VDF)). In KOH aqueous solutions, electrodes containing different binders showed quite different properties. The PE-containing electrode showed the highest capacity retention up to 14 cycles (330 mAh g^{-1}, 82.7%). However, capacity fading was observed subsequently, and only 24.6% capacity remained after 30 cycles. In contrast, the PTFE-containing electrode showed continuous capacity fading but the best capacity retention of 38.6% after 30 cycles. Comparing the amount of dropout Fe$_2$O$_3$ from electrodes after charge/discharge measurements, it was reasonable to find that the electrodes with better cycling performance showed less Fe$_2$O$_3$ dropout. When K$_2$S additives were applied, both the electrodes fabricated with PTFE and PE showed superior cycling performance, which was attributed to the good stability of PTFE and PE binders. However, when the effect of the K$_2$S additive on the Fe$_2$O$_3$ dropout was studied with PTFE-containing electrodes, heavier Fe$_2$O$_3$ dropout was observed in the K$_2$S-added electrolyte. This indicated that Fe$_2$O$_3$ dropout was not a dominant factor for the capacity fading of the electrodes.

1. Introduction

Batteries have become necessities in our daily life, and extensive research on batteries has been carried out to accommodate the current evolution of portable digital technology. Among various batteries, metal/air batteries have attracted the attention of many researchers because of their high energy density [1–3]. The anode material is the most important factor for the performance of metal/air batteries. Many candidates for anodes have been reported, such as iron [4], zinc [5–7] and aluminum [8–10]. However, zinc and aluminum anodes have some congenital disadvantages. Zinc/air primary batteries have been put to practical use in acoustic instruments, but the zinc anodes have a short cycle life in secondary batteries because of dendrite generation during cycling [7]. At the same time, non-uniform zinc dissolution and limited solubility also cause problems for its practical application. Aluminum is difficult to be used as an anode in alkaline solutions due to the protective oxide film formed on the metal surface [8,9]. In contrast, iron anodes have little problem with dendrites, and are rechargeable in alkaline aqueous solutions [3,11–26]. Batteries composed of iron anodes and an alkaline electrolyte, such as iron/air batteries, have attracted much attention due to their low cost, safety, high theoretical capacity and elemental abundance in nature.

However the use of iron anodes still suffers a number of problems. Hydrogen evolution is the most significant one for practical application of Fe$_2$O$_3$ electrodes in alkaline aqueous solutions. The potentials of the reduction reaction of Fe/Fe(OH)$_2$ and hydrogen evolution are very close [12,13], and the overpotential of hydrogen evolution on iron surfaces is small [13,14]. It was even reported that the potential of the reduction reaction of Fe/Fe(OH)$_2$ was slightly more negative than that of hydrogen evolution in an alkaline aqueous solution [12,15]. Thus, during the charging process, reactions for both the reduction of Fe/Fe(OH)$_2$ and the evolution of H$_2$ proceed simultaneously [12,15]. In our previous work, we reported that hydrogen evolution could be depressed by carbon materials such as acetylene black (AB) used as electrode additives [16,17]. It was revealed that the actual surface area of the carbon had an effect on the process of hydrogen evolution [17]. We also reported that hydrogen evolution was inhibited by FeS additives in the electrode or K$_2$S additives in the electrolyte [18,19]. The chemical adsorption of S^{2-} additives on an iron anode obstructed hydrogen evolution

∗ Corresponding author. Tel.: +81 92 583 7791; fax: +81 92 583 7791.
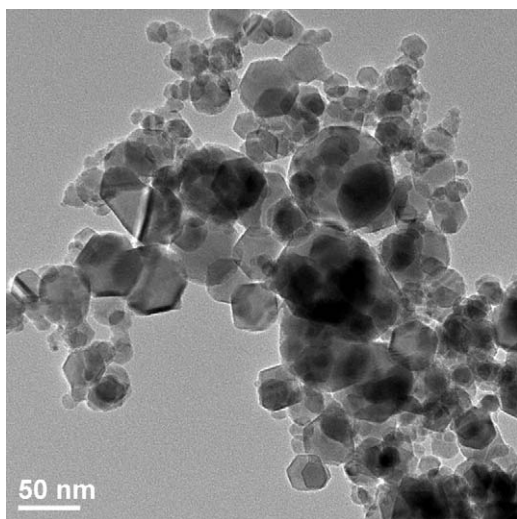E-mail address: zhaolw@cm.kyushu-u.ac.jp (L. Zhao).

Fig. 1. TEM image of nanosized Fe_2O_3 powder.

Fig. 2. Structural formulas of (a) PTFE, (b) PVDF, (c) PE, and (d) P(TFE-VDF).

[15,20]. However, although many methods have been investigated, it has been proved that it is impossible to prevent hydrogen evolution completely. Beside of the depressing effect on the charging efficiency of the electrode, hydrogen evolution is also suspected to peel particles of active materials from the electrode into the electrolyte, which induces active material dropout, and capacity fading accordingly. Therefore, electrode binders with superior adhesion property were expected to be able to prevent active materials dropout.

In the present study, we investigated the effect of binder materials on the cycling performance of Fe_2O_3 electrodes. Four materials were applied as binders—polytetrafluoroethylene (PTFE), polyvinylidene fluoride (PVDF), polyethelene (PE), and poly tetrafluoroethylene-co-vinylidene (P(TFE-VDF))—and the amount of dissolved and dropout Fe_2O_3 from the electrode containing different binders was compared. The effect of K_2S additives in the electrolyte on the electrochemical characteristics of the Fe_2O_3 electrodes fabricated with different binders was also studied.

2. Experimental

Nanosized Fe_2O_3 (Aldrich, <50 nm) was used as iron source in the present work. A typical TEM (JEOL JEM-2100F, 200 kV) image of the Fe_2O_3 powder is shown in Fig. 1. Fe_2O_3/C composite was prepared by dry-type ball milling for 24 h with 50 wt.% Fe_2O_3 powder and 50 wt.% acetylene black (AB, Denki Kagaku Co. Ltd.), which had been characterized in our previous work [18]. The products were then characterized by X-ray diffraction (XRD, RINT2100, Rigaku) with Cu K_α radiation (50 kV, 300 mA) at a scan rate of $0.5°$ min^{-1}.

The Fe_2O_3 electrodes were fabricated by mixing 90 wt.% Fe_2O_3/C composite powder with 10 wt.% binder. Four kinds of materials were used as binders, including polytetrafluoroethylene (PTFE, Daikin Co.), polyvinylidene fluoride (PVDF, Kureha Co.), polyethelene (PE, Sumitomo Chemical Co.), and poly tetrafluoroethylene-co-vinylidene (P(TFE-VDF), Daikin Co.), with average molecular weights of 4–5×10^6, 3×10^5, 1×10^5, and 0.3–1×10^5, respectively. The structural formulas of the binders are shown in Fig. 2. The Fe_2O_3 electrode with PTFE was fabricated as a pellet-type electrode. It was fabricated by mixing the Fe_2O_3/C composite powder with a 10 wt.% PTFE binder and punching in the form of disk (ca. 20 mg in weight and 10 mm in diameter). The Fe_2O_3 electrodes with PVDF, PE and P(TFE-VDF) binder were fabricated as sheet-type electrodes. They were fabricated by slurry-coating a mixture of Fe_2O_3/C composite and 10 wt.% binder (PVDF, PE

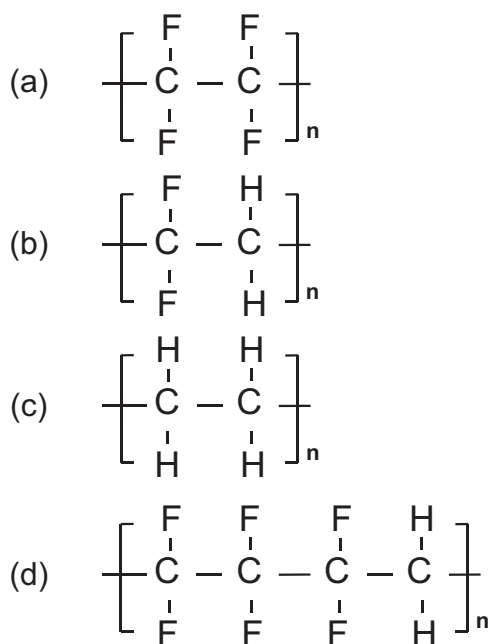and P(TFE-VDF)) in 1-methyl-2-pyrrolidinone (NMP, Wako) onto a SUS304 foil. The drying condition was 12 h at 120 °C in air in the case of PE binder, and 12 h at 80 °C in vacuum in the case of PVDF and P(TFE-VDF) binder. Then hydraulic pressing was performed on circular discs punched from the foil.

To investigate the effect of binders on the electrochemical properties of the electrodes, charge/discharge measurements were carried out in three-electrode glass cells with Pt mesh as the counter electrode and Hg/HgO as the reference electrode. The electrolyte was 25 ml 8 mol dm^{-3} KOH aqueous solution with or without 0.01 mol dm^{-3} K_2S additive. In the charging process, a coulostatic process with a cutoff capacity of 1007 mAh g^{-1}-Fe_2O_3 was carried out. In the discharge process, a galvanostatic process was performed with a cutoff potential of −0.1 V. Charge current densities were 0.5 mA cm^{-2} or 5.0 mA cm^{-2}, and discharge current densities were 0.2 mA cm^{-2} or 2.0 mA cm^{-2}.

The amount of dropout Fe_2O_3 from the electrode during cycling was analyzed quantitatively by atomic absorption spectroscopy (AAS, Hitachi High-Technologies Co., Z-5310). After 30 charge/discharge cycles, the glass cell was dissembled, and the electrolyte was introduced to AAS analysis to obtain the Fe concentration in the electrolyte after cycling. Then, based on the electrolyte volume, the amount of dissolved Fe in the electrolyte (during cycling) was obtained. After that, hydrochloric acid was added to the electrolyte to dissolve the dropout Fe_2O_3, which was deposited as particles in the glass cell during cycling. Then the solution was introduced to AAS analysis to obtain the total amount of Fe disengaged from the Fe_2O_3/C electrode during cycling. As the total amount of Fe included both dissolved Fe and dropout Fe and the amount of dissolved Fe was known, the amount of dropout Fe_2O_3 could be determined.

3. Results and discussion

The XRD patterns of the pristine Fe_2O_3 powder and the as-prepared Fe_2O_3/C composite are presented in Fig. 3. Obviously the XRD pattern of the latter matched well with that of the former, which indicated that no phase was changed via ball-milling composting, so Fe_2O_3 phase was indeed present together with carbon in the composite. On the other hand, the FWHM of the diffraction
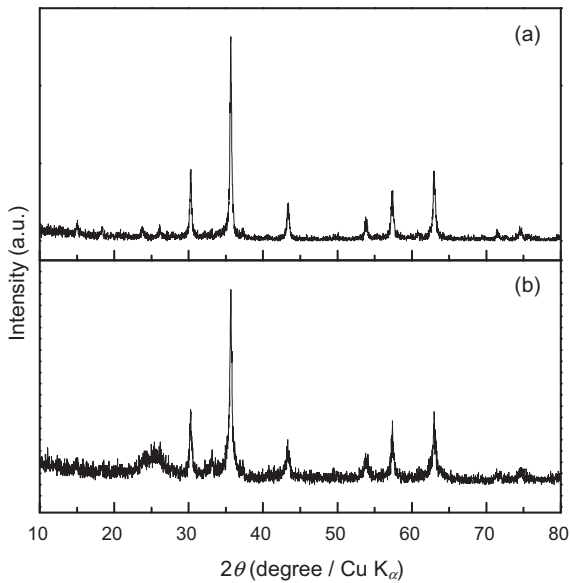
Fig. 3. XRD profiles of (a) Fe_2O_3 powder and (b) Fe_2O_3/C composite powder.

Fig. 5. Cycling performance of Fe_2O_3 electrodes fabricated with PTFE, PVDF, PE, and P(TFE-VDF) in KOH aqueous solutions.

peaks of the Fe_2O_3/C composite were slightly larger than that of the pristine Fe_2O_3. This might suggest a smaller approximate crystalline size of Fe_2O_3 in the composite.

Charge/discharge measurements were carried out to study the effect of binder materials on the electrochemical properties of Fe_2O_3 electrodes. Fig. 4 shows the charge/discharge curves of Fe_2O_3 electrodes fabricated with various binders. The electrolyte was 8 mol dm^{-3} KOH aqueous solution. Obviously, the charge/discharge curves differed according to binder content. In the discharge curves of Fe_2O_3 electrodes fabricated with PTFE and PVDF, only one plateau at around -0.8 V was observed during discharge (Fig. 4a and b). On the other hand, two plateaus at around -0.8 and -0.9 V were observed during discharge in the charge/discharge curves of Fe_2O_3 electrodes fabricated with PE and P(TFE-VDF) (Fig. 4c and d). According to prior references [20–24], the reactions of the Fe_2O_3
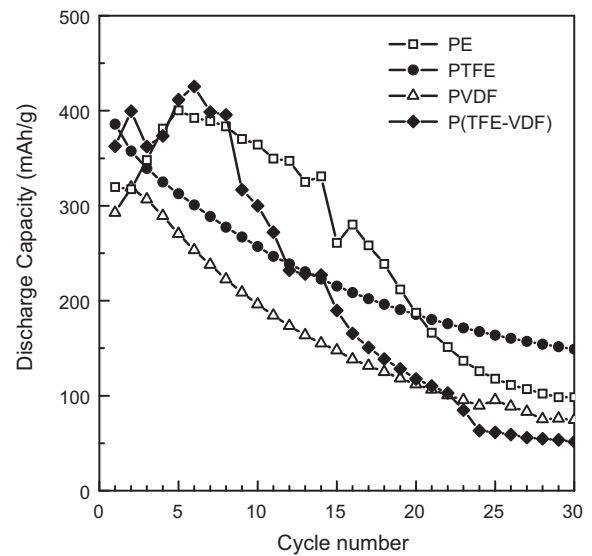
electrode in alkaline aqueous electrolyte at the first charge are:

$$Fe_2O_3 + 3H_2O + 2e^- \rightarrow 2Fe(OH)_2 + 2OH^-$$

$$and\ Fe(OH)_2 + 2e^- \rightarrow Fe + 2OH^-$$
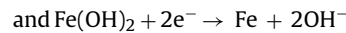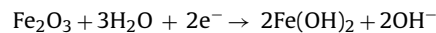
The oxidation reactions of the iron anode in alkaline solutions have been reported as the follows:

$$Fe + 2OH^- \rightarrow Fe(OH)_2 + 2e^-, \quad E_0 = -0.975\ V vs.Hg/HgO \qquad (1)$$

$$Fe(OH)_2 + OH^- \rightarrow FeOOH + H_2O + e^-,$$
$$E_0 = -0.658\ V vs.Hg/HgO \qquad (2)$$

and/or

$$3Fe(OH)_2 + 2OH^- \rightarrow Fe_3O_4 + 4H_2O + 2e^-,$$
$$E_0 = -0.758\ V vs.Hg/HgO \qquad (3)$$

Theoretically, the plateau around -0.9 V during discharge can be attributed to Eq. (1), while the one around -0.8 V can be attributed to Eq. (2) or Eq. (3). Therefore, it could be deduced that the active materials in a Fe_2O_3 electrode fabricated with PTFE or PVDF could not be reduced to Fe, while those in the electrodes fabricated with PE or P(TFE-VDF) could be. As the reduction reaction from $Fe(OH)_2$ to Fe(0) and hydrogen evolution proceeded simultaneously during the charge process [12,14], the former might be badly depressed by the latter if the hydrogen evolution happened at a more positive potential on the electrodes. Therefore, it was supposed that binder contents had an effect on the hydrogen overpotential of Fe_2O_3 electrodes.

Fig. 5 shows the cycling performance of Fe_2O_3 electrodes fabricated with various binders. The Fe_2O_3 electrode fabricated with PE showed increasing discharge capacity from 320 to 400 mAh g^{-1} in the initial 5 cycles. And within 15 cycles, the PE-containing electrode presented the best cycling performance among all four kinds of electrodes. This phenomenon was attributed to the superior adhesion properties of PE compared with other binder materials. However, capacity fading was observed subsequently, and only 24.6% capacity remained after 30 cycles. The P(TFE-VDF)-containing electrode showed similar cycling performance to that of the PE-containing one, but the capacity fading happened more early and badly. The initial discharge capacity was 363 mAh g^{-1}, and
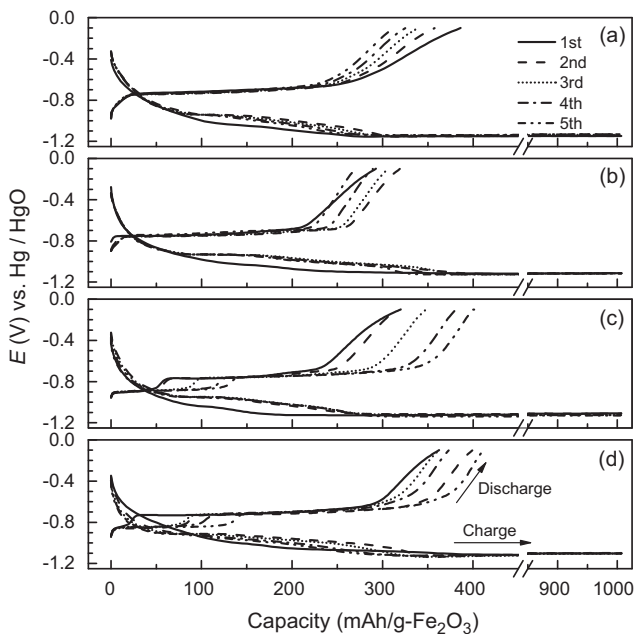

Fig. 4. The charge/discharge curves of Fe_2O_3 electrodes fabricated with (a) PTFE, (b) PVDF, (c) PE, and (d) P(TFE-VDF) in KOH aqueous solutions.
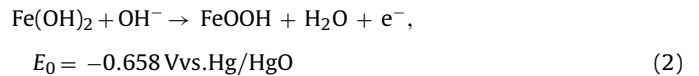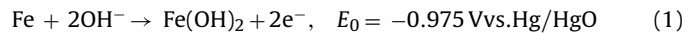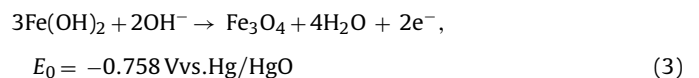
Table 1
Amounts of dropout Fe_2O_3 in alkaline solutions after 30 charge/discharge cycles.

Binder	Initial Fe_2O_3 in electrodes	Dissolution	Dissolution + dropout	Dropout Fe_2O_3
PTFE	13.2 mg	0.141 mg (1.1%)	0.655 mg (5.0%)	0.514 mg (3.9%)
PVDF	1.12 mg	0.069 mg (6.2%)	0.242 mg (21.6%)	0.173 mg (15.4%)
PE	1.68 mg	0.120 mg (7.1%)	0.182 mg (10.9%)	0.062 mg (3.8%)
P(TFE-VDF)	2.07 mg	0.127 mg (6.1%)	0.286 mg (13.8%)	0.159 mg (7.7%)

($x.x$%) is the mass ratio of the detected Fe_2O_3 by AAS to the initial Fe_2O_3.

arrived at the maximum value of 425 mAh g^{-1} at the 6th cycle. The discharge capacity decreased rapidly within 10 cycles, and finally dropped to only 56 mAh g^{-1} at the 30th cycle. In contrast, although the Fe_2O_3 electrode fabricated with PTFE showed a continuous decrease of discharge capacity from the first cycle, it presented the best cycling performance after 30 cycles with 38.6% capacity retention. As to the PVDF-containing electrode, due to the poor stability of PVDF in the strong aqueous solution, the discharge capacity decreased much faster than that of the PTFE-containing electrode.

To evaluate the adhesion property of binders, the amount of dropout Fe_2O_3 in the electrolytes after 30 cycles with different electrodes was compared. It was suggested that binders with superior adhesion property could prevent active materials in the electrode from dropping into the electrolyte. Thus, not the amount of dissolution but the amount of dropout Fe_2O_3 was compared. The results are shown in Table 1. These results proved that dropout Fe_2O_3 existed in the electrolytes. Comparing the ratios (%) of the amount of dropout Fe_2O_3 to the initial amount of Fe_2O_3, we found that the amount of dropout Fe_2O_3 from the electrodes fabricated with PTFE and PE was small. The ratio of dropout Fe_2O_3 from electrodes fabricated with PVDF was the largest, at 15.4%, and that fabricated with P(TFE-VDF) was the second largest, at 7.7%. In contrast, the ratio of dropout Fe_2O_3 from electrodes fabricated with PTFE or PE was 3.9% or 3.8%, respectively. The reason was supposed to be that PTFE and PE has superior adhesion properties to PVDF and (P(TFE-VDF)) binders. Accordingly, larger masses of electrodes are obtained with PTFE or PE binder. As both hydrogen evolution and Fe_2O_3 dropout mainly occur at the geometric surface of the electrode, more massive electrode, (with PTFE or PE binder,) was advantageous, in particular via the comparison based on gravimetric ratio. Comparing the data from Table 1 with that from Fig. 5, it was reasonable to find that the electrode with better cycling performance showed less Fe_2O_3 dropout. This finding indicated that the Fe_2O_3 dropout was a non-negligible factor for the capacity fading of the electrode.

It has been reported [18,19,25,26] that the electrochemical properties of an iron negative electrode was improved by K_2S additives in the alkaline electrolyte. So charge/discharge measurements were also carried out in order to investigate the effect of binder contents on the iron negative electrodes in KOH + K_2S solutions. Fig. 6 shows the charge/discharge curves of Fe_2O_3 electrodes fabricated with various binders in KOH aqueous solutions with K_2S additives. Compared with results without K_2S additives, the discharge capacities of all Fe_2O_3 electrodes fabricated with various binders in KOH + K_2S solutions were increased significantly. These increases mainly corresponded to the change of the plateaus at −0.9 V, attributed to Eq. (1). Especially in the case of the PTFE and PVDF binders, major differences were found between the discharge curves with and without K_2S additives. The plateau at around −0.9 V during discharge was not observed without K_2S in Fig. 4a and b, but did appear with the K_2S additive in Fig. 6a and b. Also in the case of PE and P(TFE-VDF) binder, the plateau at around −0.9 V during discharge became larger. It was reported that S^{2-} was absorbed on the electrode/electrolyte interface and then the molecular recombination reaction of hydrogen was inhibited by S^{2-} ion chemisorption [25], and the change in surface species likely
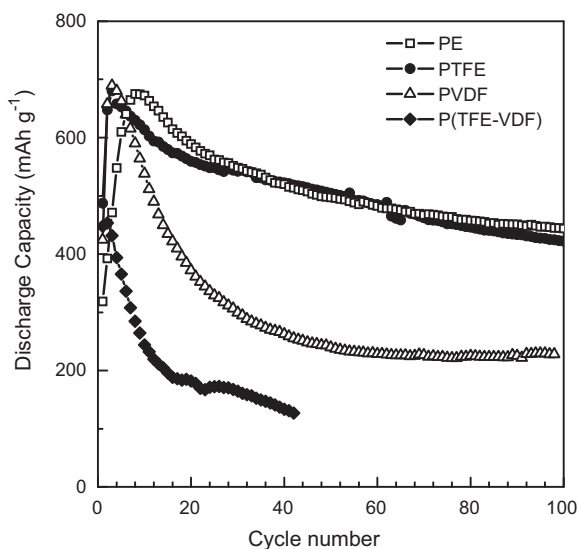
influences the overpotential of hydrogen evolution [27]. Therefore, hydrogen evolution was prevented, and the reduction reaction from $Fe(OH)_2$ to Fe proceeded, then the discharge capacity of the oxidation reaction from Fe to $Fe(OH)_2$ was increased.

Also, the discharge capacity of all Fe_2O_3 electrodes fabricated with various binders in KOH aqueous solutions with K_2S additives increased up to the 3rd cycle. In the case of the Fe_2O_3 electrode fabricated with PTFE, the discharge capacity was 488 mAh g^{-1} at the 1st cycle and increased to 648 mAh g^{-1} at the 2nd cycle and 680 mAh g^{-1} at the 3rd cycle. S^{2-} was absorbed on the electrode/electrolyte interface. It was anticipated that this chemical absorption of sulfur ions interfered with the dissolution and deposition reaction of the iron anode in the initial 3 cycles. And the surface of electrode might have changed to a more suitable condition for a dissolution and deposition reaction after that. In the case of the electrode fabricated with PE binder, the increase of discharge capacity lasted up to 5 cycles as shown in Fig. 6c, which was similar to the result obtained with the KOH aqueous electrolyte before K_2S was added.

Fig. 7 shows the cycling performances of Fe_2O_3 electrodes fabricated with various binders in KOH aqueous solutions with K_2S additives. These results showed that Fe_2O_3 electrodes fabricated with PTFE and PE have superior cycling performances. The maximum discharge capacity of Fe_2O_3 electrodes fabricated with PTFE and PE was 680 mAh g^{-1} at the 3rd cycle and 675 mAh g^{-1} at the 8th cycle, respectively. After 30 cycles, the electrodes fabricated with PTFE and PE presented good cycling performance with 79.7% and 81.3% capacity retention, respectively. This is likely due to the good stability of PTFE and PE binders in alkaline solution.
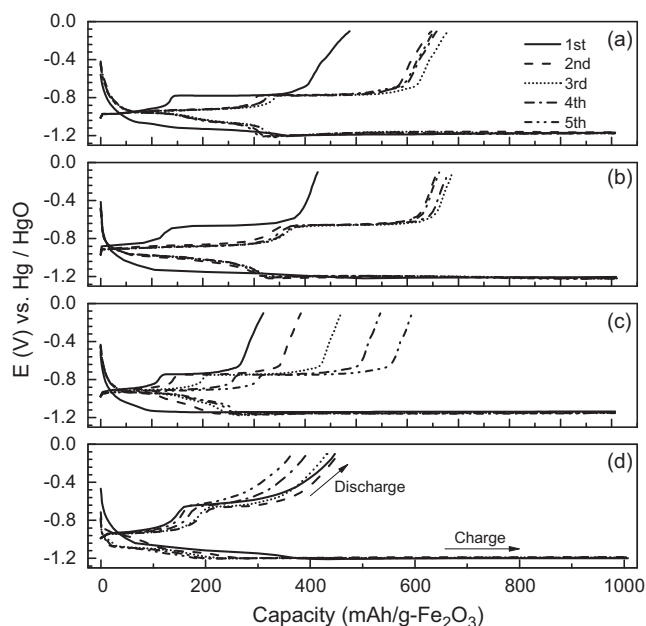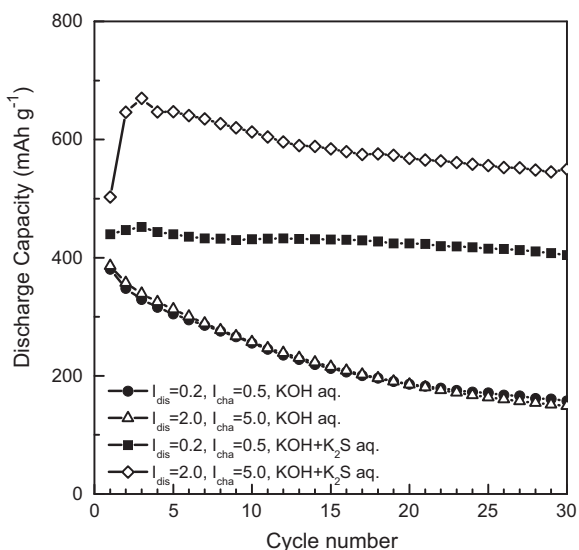

Fig. 6. The charge/discharge curves of Fe_2O_3 electrodes fabricated with (a) PTFE, (b) PVDF, (c) PE, and (d) P(TFE-VDF) in KOH aqueous solutions with K_2S additives.

Fig. 7. Cycling performance of Fe_2O_3 electrodes fabricated with PTFE, PVDF, PE, and P(TFE-VDF) in KOH aqueous solutions with K_2S additives.

Table 2
Amounts of dropout Fe_2O_3 from electrodes fabricated with PTFE after 30 charge/discharge cycles under different conditions.

Electrolyte	Current density (mA cm^{-2})		Dropout Fe_2O_3
	Charge	Discharge	
KOH	0.5	0.2	0.514 mg (3.9%)
KOH	5.0	2.0	0.476 mg (3.5%)
KOH + K_2S	0.5	0.2	1.399 mg (13.0%)
KOH + K_2S	5.0	2.0	0.794 mg (6.7%)

(x.x%) is the mass ratio of the detected Fe_2O_3 by AAS to the initial Fe_2O_3.

In contrast, Fe_2O_3 electrodes fabricated with PVDF or P(TFE-VDF) had poor cycle life. As for PVDF, the maximum discharge capacity of the electrode was 689 mAh g^{-1}, which was the largest discharge capacity in four electrodes fabricated with various binders. However, capacity fading was observed within 20 cycles, and only 43.4% capacity was maintained after 30 cycles. This was caused by decomposition of PVDF in strong alkaline solution. P(TFE-VDF) had been expected to be a more stable binder than PVDF in strong alkaline solutions. However, the maximum discharge capacity (454 mAh g^{-1}) and capacity retention after 30 cycles (36.2%) was even worse. From these results, it was revealed that PTFE and PE were the most suitable binders for the Fe_2O_3 negative electrode, because of their stability in strong alkaline solution and superior adhesion properties.

To investigate the effect of the K_2S electrolyte additive on the process of Fe_2O_3 dropout, detailed studies were carried out on PTFE-containing electrodes at different electrochemical cycling conditions. Fig. 8 shows the cycling results of the electrodes in the electrolyte with or without K_2S additives under different conditions. As expected, the capacity retention of the electrode was greatly improved by K_2S additives regardless of the variations of cycling current density. The amounts of dropout Fe_2O_3 from the PTFE-containing electrode after cycling under different conditions are compared in Table 2. Contrary to our expectations, the amount of Fe_2O_3 dropout increased from 3.9% to 13.0% and 3.5% to 6.7%, respectively, when K_2S additive was used. This result seems to be contrary to the above conclusion from Table 1 that the Fe_2O_3 dropout had a direct relationship with electrode capacity fading. However, if we compare the data obtained with the same electrolyte, the conclusion from Table 1 still works well. In KOH aqueous solutions, the results of dropout Fe_2O_3 measured at different current densities were quite similar, consistent with the results of cycling performance in KOH aqueous solutions. When K_2S additives were applied, the amount of dropout Fe_2O_3 measured at higher current density was smaller than that at lower current densities. Accordingly, much better capacity retention was obtained with higher current density. Therefore, it was revealed that the Fe_2O_3 electrodes showing a small amount of dropout Fe_2O_3 had superior cycling performances in the same electrolyte. As this relationship did not work when the electrolyte was different, it was suggested that the capacity decrease was caused not only by electrode dropout for hydrogen evolution but also by other processes, and/or the Fe_2O_3 dropout was also affected by some other factors in spite of hydrogen evolution. For example, in KOH + K_2S electrolyte, the Fe_2O_3/C electrode showed larger discharge capacity than that in KOH electrolyte. This indicated a better utilization of Fe_2O_3 particles in KOH + K_2S electrolyte during cycling. Therefore, a larger volume change was expected for the Fe_2O_3 in KOH + K_2S electrolyte, which might be the reason for the stronger Fe_2O_3 dropout in the electrolyte.

4. Conclusions

The effects of binders PTFE, PVDF, PE and P(TFE-VDF) on the electrochemical properties of Fe_2O_3 electrodes were investigated. In KOH aqueous solutions, the PE-containing Fe_2O_3 electrode showed the highest discharge capacity retention of the four candidates up to 14 cycles (330 mAh g^{-1}, 82.7%). However, the discharge capacity began to decrease after 15 cycles; by contrast, the PTFE-containing electrode showed continuous capacity fading but the best capacity retention of 38.6% after 30 cycles. A comparison of the dropout Fe_2O_3 was carried out after charge/discharge measurements. The electrodes fabricated with PTFE or PE showed less Fe_2O_3 dropout than those fabricated with PVDF or P(TFE-VDF). It was reasonable to find that the electrodes with better cycling performance showed less Fe_2O_3 dropout. When K_2S additives were applied, both the electrodes fabricated with PTFE and PE showed superior cycling performance with 79.7% and 81.3% capacity retention after 30 cycles, respectively. This was attributed to their good stability in strong alkaline solutions and superior adhesion properties. Therefore, PTFE and PE were concluded to be the most suitable binders for Fe_2O_3 negative electrodes in alkaline aqueous solutions. However,

Fig. 8. Cycling performance of Fe_2O_3 electrodes fabricated with PTFE under different conditions.

when the effect of K_2S additive on the Fe_2O_3 dropout was studied with PTFE-containing electrodes, heavier Fe_2O_3 dropout was observed in the K_2S-added electrolyte. This indicated that Fe_2O_3 dropout was not a dominant factor for the electrode capacity fading.

Acknowledgment

References

[1] D. Linden, T.B. Reddy, Handbook of Batteries, third ed., McGraw-Hill, New York, 2002.
[2] H. Arai, M. Hayashi, Encyclopedia of Electrochemical Power Sources, fourth ed., Elsevier B.V., Amsterdam, 2009, p. 347.
[3] K.F. Blurton, A.F. Sammells, J. Power Sources 4 (1979) 263–279.
[4] L. Ojefors, L. Carlsson, J. Power Sources 2 (1977–1978) 287–296.
[5] C. Chakkaravarthy, A.K. Abdul Waheed, H.V.K. Udupa, J. Power Sources 6 (1981) 203–228.
[6] S. Muller, F. Holzer, O. Haas, J. Appl. Electrochem. 28 (1998) 895–898.
[7] M. Ma, J.P. Tu, Y.F. Yuan, X.L. Wang, K.L. Li, F. Mao, Z.Y. Zeng, J. Power Sources 179 (2008) 395–400.
[8] Q. Li, N.J. Bjerrum, J. Power Sources 110 (2002) 1–10.
[9] V. Kapali, S.V. Iyer, V. Balaramachandran, K.B. Sarangaoani, M. Ganesan, M.A. Kulandainathan, A.S. Mideen, J. Power Sources 39 (1992) 263–269.
[10] S. Yang, H. Knickle, J. Power Sources 112 (2002) 162–173.
[11] K. Micka, Z. Zabransky, J. Power Sources 19 (1987) 315–323.
[12] A.K. Shukla, M.K. Ravikumar, T.S. Bapasubramanian, J. Power Sources 51 (1994) 29–36.
[13] P. Periasamy, B.R. Bahu, S.V. Iyer, J. Power Sources 62 (1996) 9–14.
[14] K. Vijayamohanan, T.S. Balasubramanian, A.K. Shukla, J. Power Sources 34 (1991) 269–285.
[15] C. Chakkaravarthy, P. Periasamy, S. Jegannathan, K.I. Vasu, J. Power Sources 35 (1991) 21–35.
[16] B.T. Hang, T. Watanabe, M. Egashira, S. Okada, J. Yamaki, S. Hata, S. Yoon, I. Mochida, J. Power Sources 150 (2005) 261–271.
[17] B.T. Hang, M. Egashira, I. Watanabe, S. Okada, J. Yamaki, S. Yoon, I. Mochida, J. Power Sources 143 (2005) 256–264.
[18] B.T. Hang, T. Watanabe, M. Egashira, I. Watanabe, S. Okada, J. Yamaki, J. Power Sources 155 (2006) 461–469.
[19] B.T. Hang, S.-H. Yoon, S. Okada, J. Yamaki, J. Power Sources 168 (2007) 522–532.
[20] P. Periasamy, B.R. Babu, S.V. Iyer, J. Power Sources 63 (1997) 79–85.
[21] R.D. Armstrong, I. Baurhoo, J. Electroanal. Chem. 40 (1972) 325–338.
[22] A.J. Salkind, C.J. Venuto, S.U. Falk, J. Electrochem. Soc. 111 (1964) 493–495.
[23] L. Ojefors, J. Electrochem. Soc. 123 (1976) 1691–1696.
[24] P. Periasamy, B.R. Babu, S.V. Iyer, J. Power Sources 58 (1996) 35–40.
[25] R. Carta, S. Demini, A.M. Polcaro, P.F. Ricci, G. Tola, J. Electroanal. Chem. 251 (1988) 257–268.
[26] L. Ojefors, Electrochim. Acta 21 (1976) 263–266.
[27] R.S. Schrebler-Guzman, J.R. Viche, A.J. Arvia, Electrochim. Acta 24 (1979) 395–403.